Autonomous Underwater Vehicle Localization using an Extended Kalman Filter

ROSA, Daniel
dgd.rosa@gmail.com
IST id: 90041

RIBEIRO, Diogo
diogoribeiro0015@gmail.com
IST id: 90051

HONRADO, Duarte
duartehonrado@gmail.com
IST id: 90058

VIEGAS, Guilherme
ggmviegas@gmail.com
IST id: 90090

August 29, 2024

***Abstract*—This report addresses the problem of underwater localization of an autonomous underwater vehicle (AUV) using the Extended Kalman Filter (EKF). The EKF approach consists on the linearization of both the system model and the measurement model around the values of the state variables on each iteration. An USBL sensor is used for the localization together with a beacon with an acoustic modem. The results of realistic simulations done with the Gazebo simulator illustrate the localization performance achieved with the proposed solution, when compared with a dead reckoning approach where the AUV localization is estimated only through the system model.**

***Keywords*—** EKF, AUV, USBL

II. Introduction

The world of autonomous robots as seen great advances for the few last decades. This advances were possible due to further research in some key robotic areas such as mapping, motion planning and the key aspect that is the focus of this work - Localization.

Localization is the process of determining where a robot is located with respect to its environment. To produce good representations of the world or to plan realistic motion plans one shall have first the capability of localizing itself in the best possible way.

Localizing a robot, or more specifically, knowing the position and attitude of a robot with respect to a defined frame, is a known problem in robotics. This problem is mainly due to the imperfections of the real world. Sensors produce noisy measurements and actuators do not produce the exact movements that are defined in a theoretical motion model.

As so, taking into account this uncertainty is very important to produce good estimates of the robot's pose. Some ways exist to produce these estimates, being one of them the application of a Kalman filter.

Based on the Bayes theorem, the Kalman Filter estimates hidden variables based on inaccurate measurements and provides predictions of the future system state based on past estimations. Although an optimal estimator, this optimality is only possible for problems with both the system's and measurement's models governed by linear equations.

As in this work's case both the model of the system and the model of observations are nonlinear, some changes have to be made to the common Kalman filter in order to produce good estimates for the robot's pose. This work studies the application of the Extended Kalman Filter (EKF), where both the motion and measurement model are linearized, at each timestep, around the current mean and error covariance of the system's state.

The objective of this project is to do the localization of an Autonomous Underwater Vehicle (AUV), resorting to an EKF. For the execution of this task, an ultra-short-baseline sensor (USBL) will be used together with a beacon equipped with an acoustic modem. The position of the beacon is known apriori and through acoustic signals, the USBL will gather information about its position. Based on this measurements, the EKF will produce an estimation of the vehicle state along time.

The AUV and its localization were tested using a simulator built over the *UUV Simulator* [Manhães et al. 2016] and developed by the Dynamical Systems and Ocean Robotics Laboratory (DSOR), belonging to the Institute for Systems and Robotics (ISR) of the Instituto Superior Técnico (IST).

III. Problem Description

A. Problem Framework

According to Fig.1, let $\{U\}$ be the inertial frame and $\{B\}$ be the body-frame attached to the center of gravity of the vehicle. Let $\hat{\boldsymbol{x}} = [\hat{x}, \hat{y}, \hat{\psi}]$ be the estimated state of the center of $\{B\}$ in $\{U\}$. The kinematic motion model in a 2D plane is defined by

$$\begin{cases} \dot{\hat{x}} = u\cos\psi - v\sin\psi \\ \dot{\hat{y}} = u\sin\psi + v\cos\psi \\ \dot{\hat{\psi}} = r \end{cases}, \tag{1}$$

where $u \in \mathbb{R}$ and $v \in \mathbb{R}$ are the surge and sway linear speeds, respectively, of the center of $\{B\}$ in $\{U\}$, the $\psi \in \mathbb{R}$ is the heading angle of $\{B\}$ in $\{U\}$ and $r \in \mathbb{R}$ is the heading angle rate. The surge and sway are assumed to be given by the Doppler Velocity Logs sensor (DVL), besides the heading rate is attained by the Attitude and Heading Reference System (AHRS) sensor. These three variables are inputs to the positioning filter. Furthermore, ocean currents and other disturbances are not considered in the motion model.

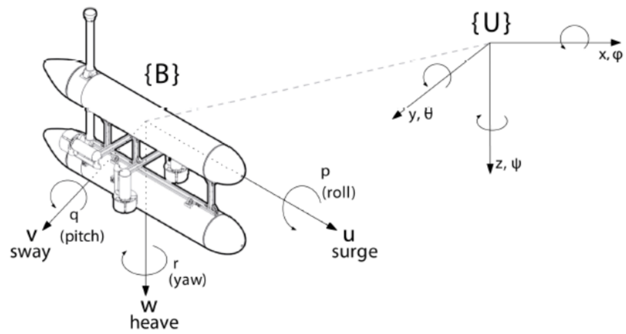

Fig. 1. Reference Frames used.

B. Process and Measurement Model

To develop the filter, it is required to define the process model and measurement model. Both can be defined as

$$\boldsymbol{x_{k+1}} = f(\boldsymbol{x_k}, \boldsymbol{u_k}) + \boldsymbol{w_k}, \tag{2}$$

$$\boldsymbol{y_k} = h(\boldsymbol{x_k}) + \boldsymbol{v_k}, \quad (3)$$

where k is a time index, $f(.) : \mathbb{R}^3 \rightarrow \mathbb{R}^3$ is a nonlinear function of the state vector $\boldsymbol{x} = [x, y, \psi]^T$ and the input vector is $\boldsymbol{u_k} = [u, v, r]^T$; $h(.)$ is a nonlinear function that generates the measurement taken at time k by the vehicle at state $\boldsymbol{x_k}$ and $\boldsymbol{y_k}$ is the measurement vector taken at time k; $\boldsymbol{w_k}$ is the process noise in the instant k which is defined by white Gaussian noise, with zero mean and constant covariance matrix Q and $\boldsymbol{v_k}$ is the measurement noise, also represented by white Gaussian noise with zero mean and constant covariance matrix R. In addition, the process noise and measurement noise are assumed to be mutually independent.

IV. Extended Kalman Filter

Since the system is nonlinear, the localization is estimated resorting to an Extended Kalman Filter. The measurement vector $\boldsymbol{y_k}$ is constituted by the USBL measurements, range, bearing and elevation, and the heading measurement by the AHRS. In Fig.2 it is possible to see a simple diagram of this work's filter approach where the EKF processes all the sensor information received through the USBL, the AHRS and the DVL and produces a pose estimation using a loop of both *prediction* and *update* steps, which are explained in more detail in section IV-B.

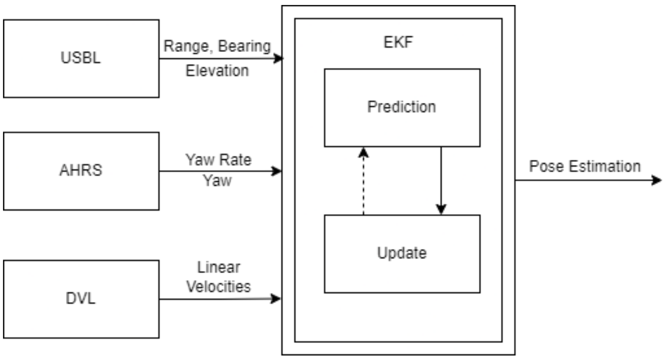

Fig. 2. Extended Kalman Filter setup

A. USBL Sensor

An ultra-short-base sensor (USBL) can be used for tracking and navigation of underwater vehicles through position triangulation, as it is possible to calculate acoustic measurements of distance and direction. The USBL sensor consists of a small and compact block of acoustic transducers that enable the computation of the transponder's position on the vehicle's coordinate frame. Furthermore, it is needed to have an acoustic modem that sends acoustics signals to the vehicle. In this work, this modem is on a beacon at surface level ($z_b = 0$) and it is known its absolute position apriori.

Each USBL measures a range R, elevation e and bearing b which are described by

$$\begin{bmatrix} R \\ e \\ b \end{bmatrix} = \begin{bmatrix} \sqrt{(x_b - x)^2 + (y_b - y)^2 + z^2} \\ \arcsin\left(\frac{-z}{\sqrt{(x_b-x)^2+(y_b-y)^2+z^2}}\right) \\ \arctan\left(\frac{y_b - y}{x_b - x}\right) \end{bmatrix} + \mathcal{N}(0, \sigma_h), \quad (4)$$

where x_b and y_b are the position of the beacon with the modem and z is the fixed depth of the vehicle, bearing in the mind the beacon is positioned at $z = 0m$.

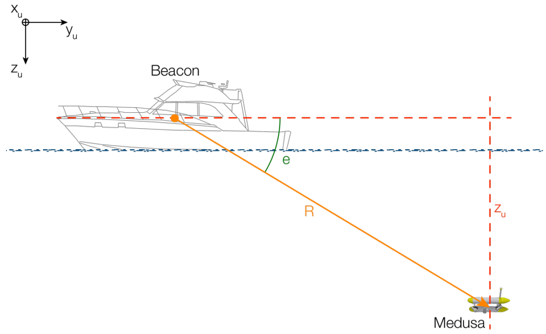

Fig. 3. UBSL range and elevation diagram - Side view

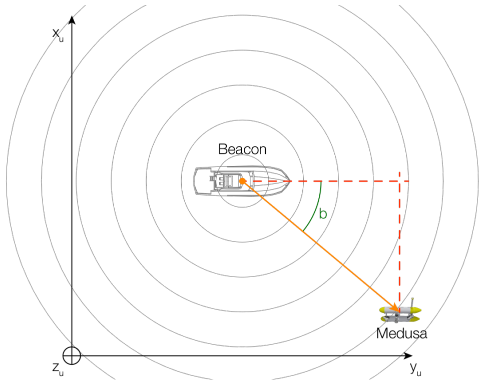

Fig. 4. USBL bearing diagram - Top view

B. Predict and Update Steps

The main components of this filter are the predict step and the update step. Looking first to the predict step, there are two main equations, one for the predicted state estimate:

$$\hat{x}_k^- = f(\hat{x}_{k-1}, u_{k-1}) \quad (5)$$

And the other for the predicted covariance estimate:

$$P_k^- = A_k P_{k-1} A_k^T + Q_k, \quad (6)$$

where $\hat{x}_k^-$ is the estimation a priori for the instant k. Now, the Update step is constituted by the following equations

$$\hat{y}_k = z_k - h(\hat{x}_k^-) \quad (7)$$

$$S_k = H_k P_k^- H_k^T + R_k \quad (8)$$

$$K_k = P_k^- H_k^T S_k^{-1} \quad (9)$$

$$\hat{x}_k = \hat{x}_k^- + K_k \hat{y}_k \quad (10)$$

$$P_k = (I - K_k H_k) P_k^-, \quad (11)$$

Eq.(7) computes the measurement residual, Eq.(8) the residual covariance, Eq.(9) the Near-optimal Kalman gain, Eq.(10) updates the state estimate, where $\hat{x}_k$ is the estimation after the measurements, and Eq.(11) updates the covariance estimate. A_k is the state matrix given by

$$A_k = \left.\frac{\partial f}{\partial x}\right|_{\hat{x}_{k-1}, u_k}, \quad (12)$$

and H_k represents the observation matrix and it is defined by the following Jacobian

$$H_k = \left.\frac{\partial h}{\partial x}\right|_{\hat{x}_k}. \tag{13}$$

C. System Linearization

Now, to use the Extended Kalman filter, one needs to linearize the process model and measurement model, as shown in equations (12) and (13). Linearizing 1 around the system's state leads to the matrix A_k

$$A_k = \begin{bmatrix} 1 & 0 & -u_k \Delta t \sin\psi_k - v_k \Delta t \cos\psi_k \\ 0 & 1 & u_k \Delta t \cos\psi - v_k \Delta t \sin\psi_k \\ 0 & 0 & 1 \end{bmatrix}, \tag{14}$$

where Δt represents the time step. The measurement model, joining both the USBL and the AHRS measurements, is described by

$$\begin{bmatrix} R \\ e \\ b \\ \psi \end{bmatrix} = \begin{bmatrix} \sqrt{(x_b - x_k)^2 + (y_b - y_k)^2 + z^2} \\ \arcsin\left(\frac{-z}{\sqrt{(x_b - x_k)^2 + (y_b - y_k)^2 + z^2}}\right) \\ \arctan\left(\frac{y_b - y_k}{x_b - x_k}\right) \\ \psi_k \end{bmatrix} + \mathcal{N}(0, \sigma_h) \tag{15}$$

Note that the heading value is given directly by the AHRS sensor. Then, its linearization around the system's state is given by

$$H_k = \begin{bmatrix} \frac{-X}{\sqrt{X^2+Y^2+z^2}} & \frac{-Y}{\sqrt{X^2+Y^2+z^2}} & 0 \\ -\frac{zX}{\sqrt{X^2+Y^2}(X^2+Y^2+z^2)} & -\frac{zY}{\sqrt{X^2+Y^2}(X^2+Y^2+z^2)} & 0 \\ -\frac{Y}{X^2+Y^2} & \frac{X}{X^2+Y^2} & 0 \\ 0 & 0 & 1 \end{bmatrix}, \tag{16}$$

with $X = x_b - x_k$, $Y = y_b - y$ and z is the depth of the AUV as the beacon is positioned at $z = 0m$.

V. Simulation Results

The performance of the proposed Extended Kalman Filter and the localization of the AUV robot are assessed using the DSOR simulator. For all tests, the plot of the EKF pose, the Ground Truth pose and the Dead Reckoning pose are plotted, as well as the covariance ellipses product of the EKF filter. Four different tests are done to assess the correctness of the implementation and to provide a wider range of results: 1) Trajectory of relatively big length, 2) Trajectory passing near the beacon, 3) Trajectory far-away from the beacon and 4) Trajectory where communications between the AUV and the beacon are disconnected for a specified period of time. For all tests the performance is evaluated comparing the differences between position estimates and ground truth position in terms of the root-mean-square-error (RMSE), using 10 samples for each trajectory "mode". Important to note that the ROS node that implements the Extended Kalman Filter works at a 10 Hz frequency, whereas the measurements from the USBL sensor are received at a 1Hz frequency. This means, in practice, that the *Update* step is done for every 9 iterations of the *Predict* step.

A. Big length trajectory

First, a lawn-mower like trajectory of a relatively big length is produced to assess if the filter implementation improves the localization estimate when compared with the dead reckoning localization. Figure 5 depicts the complete trajectory, with the beacon position at the coordinates X = 40m and Y = 20m. One can see a clear deviation between the ground truth and the dead reckoning, while the filter implementation produces a trajectory estimate closer to the ground truth. A focused view can be seen in the circle of Fig.5, where the red ellipses represent the covariance error when an *update* step of the EKF was done and the blue ellipses the covariance error one

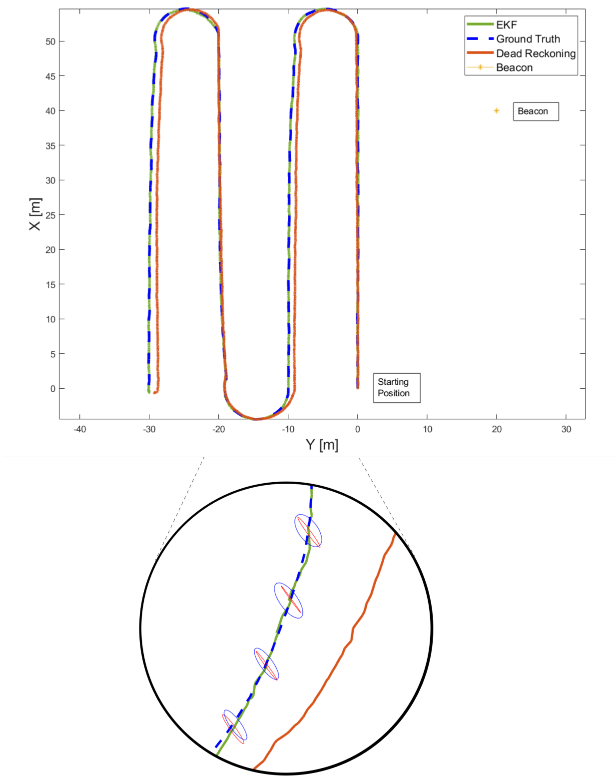

Fig. 5. Trajectory of relatively big length

iteration prior to the *update step*. Looking at both ellipses, along the trajectory, one can see that the *update* step of the filter is able to reduce the covariance error the filter had up to that instant.

Fig.6 shows the root-mean-squared-error between ground truth and both EKF and dead reckoning, clearly showing a better performance when using the filter.

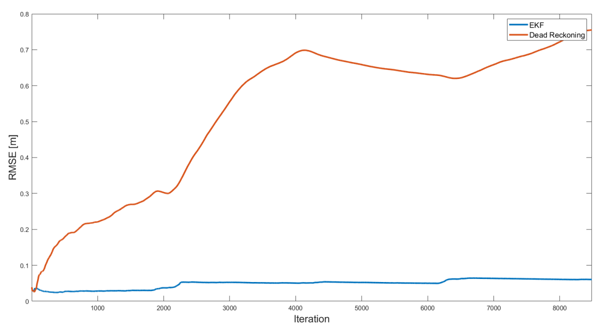

Fig. 6. RMSE - Trajectory of relatively big length

B. Near beacon

For the following three tests a smaller length trajectory was implemented to observe in more detail the different changes in the localization algorithm performance.

A test with the beacon relatively close to the trajectory was done, positioning it at X = 40m and Y = 20m. As seen in Fig.7, the trajectory remains a lawn-mower like path. Fig.8 shows the evolution of the ψ angle prediction both for the EKF and the dead reckoning with comparison to the ground truth. One can see here that, despite some small noise and a small drift from the dead reckoning, both predictions are very close to the ground truth. This can be explained by looking at the way we model the heading angle in the system's model, as the next step predictions are dependent of a heading angle input received from the AHRS sensor which is always the same value of the ground truth and therefore the correct heading angle value used in the propagation of the dead reckoning position estimates.

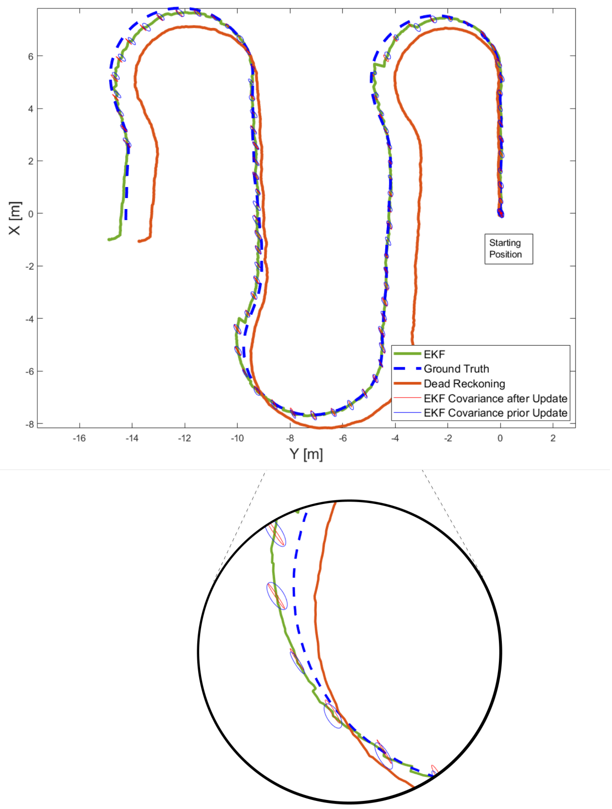

Fig. 7. Trajectory with beacon near the path

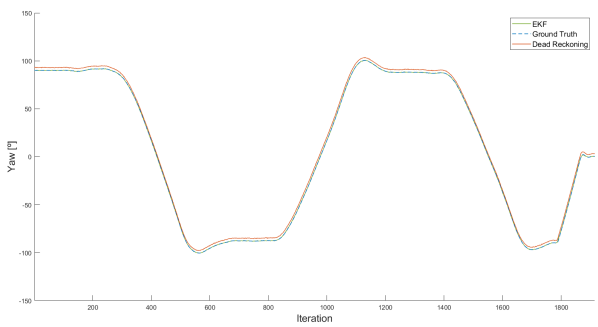

Fig. 8. ψ evolution - Trajectory near the beacon

The RMSE for the filter implementation and the dead reckoning is also presented in Fig.9, showing that the filter is capable of maintaining a close prediction of the AUV localization when compared to the growing error of the dead reckoning.

C. Far from beacon

As the measurement noise is closely related with the distance from the sensor to the AUV, a test was done moving the beacon from its original position.The beacon was moved from the position (40, 20) [m] to the position (-120, 90) [m] to test the behaviour of the

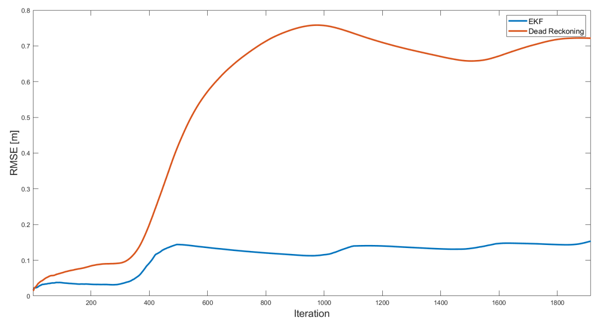

Fig. 9. RMSE - Trajectory near the beacon

EKF when the sensor gets farther away from the AUV. Although not easily seen in Fig.10 as the differences between this test and the previous one are not very pronunciated, a closer look at the root-mean-squared-error in Fig.11 shows a slight increase in the error, where it maintained almost a constant error of 0.25m when compared with the test with the beacon positioned near the path where the RMSE of the EKF remained constant at around 0.13m. This slight increase was nevertheless much better than that of the dead reckoning.

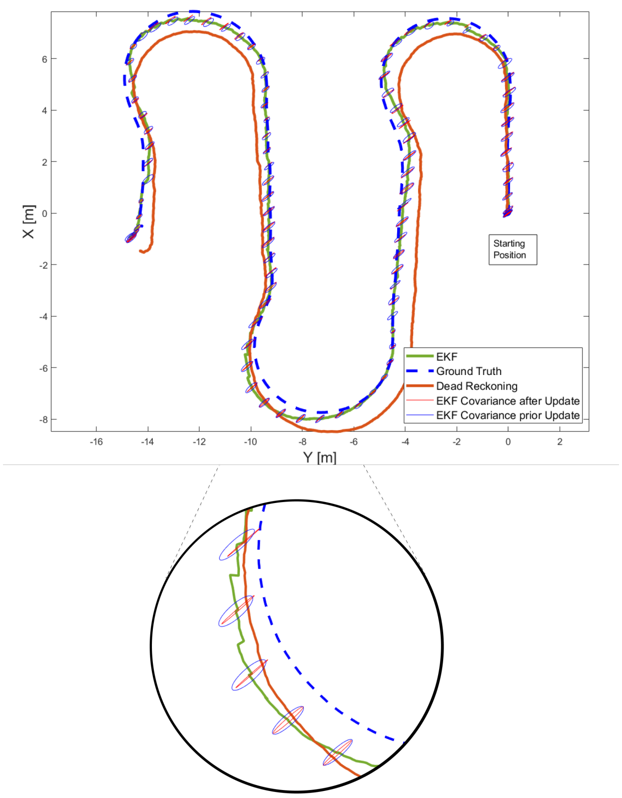

Fig. 10. Trajectory with beacon far from the path

D. Sensor communications disconnected

For the last test, the communications are disconnected from the beginning, only to be connected at iteration 800 (at almost half the trajectory). This allows to prove the convergence of the EKF to the ground truth, even when the *Update* step of the filter was disabled for a certain period of time.

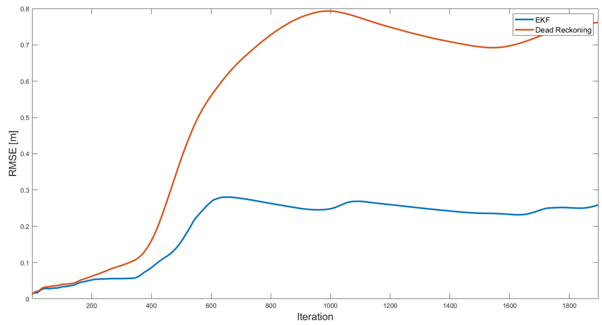

Fig. 11. RMSE - Trajectory far from the beacon

Fig.12 shows the respective predictions of the AUV localization along its motion. One can see that, as the sensor communications are disconnected, the EKF filter can only make use of the *predict* step, propagating forward its localization predictions according to the system model equations. At approximately position X = -6m and Y = -3.8m the communications were established where one is able to see the convergence of the EKF estimation to the ground truth trajectory. The focused image below shows the covariance matrices in detail, proving the reduction of the error of the covariance once the communications are established.

As seen in Fig.13, the root-mean-square error is the same for both EKF and dead reckoning up to iteration 800, as up to this point the EKF only propagates forward the state according to the process model. From the 800th iteration, the EKF rmse drops substantially when compared with the dead reckoning, proving the convergence of the EKF predictions to the ground truth when the *Update* step is activated

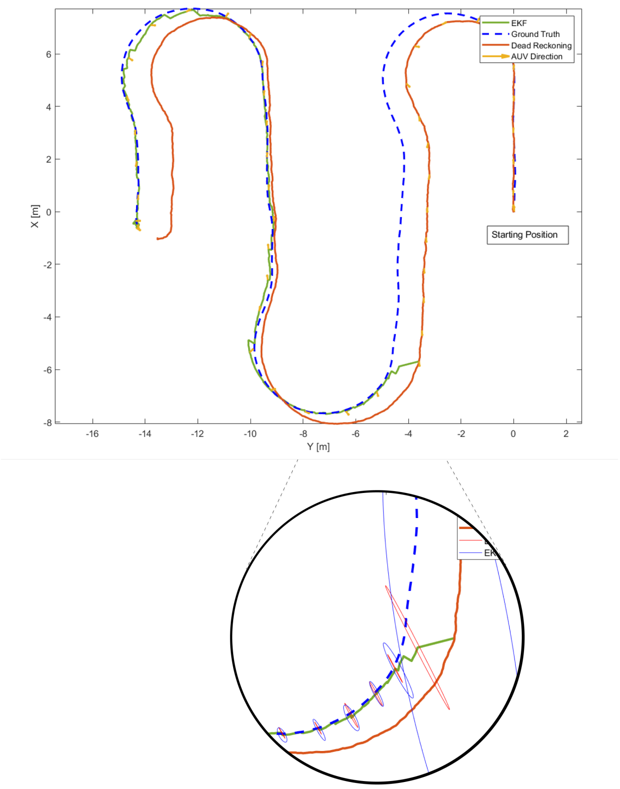

Fig. 12. Trajectory with communications disconnected

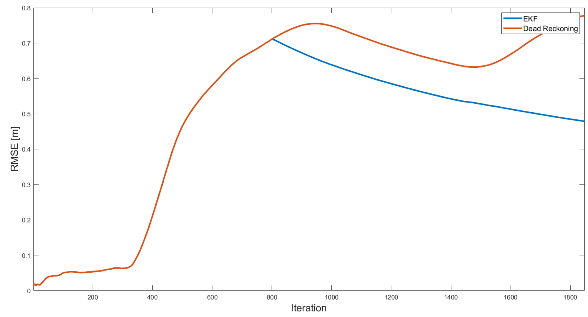

Fig. 13. RMSE - Trajectory with communications disconnected

VI. Conclusion

The problem of pose localization of an underwater autonomous vehicle was addressed in this work.

A Bayesian filter approach, namely the Extended Kalman Filter, was proposed to estimate the robot's pose along a trajectory, where the altitude was maintained at a constant level. An USBL and an AHRS sensor was used as sensors.

The proposed solution has achieved good performance at estimating the vehicle's pose when compared to the dead reckoning estimate. This performance was evaluated using 4 different tests, using the root-mean-square-error as a performance metric.

Future work includes extending the problem to the 3D domain by using a variable height for the AUV trajectory instead of just a variable length and width. Furthermore, using a dynamic model instead of just a kinematic one could be interesting as this could model, for example, ocean currents. Testing the proposed approach in a real domain should be conducted.

$$H_k = \frac{\partial h}{\partial x}\bigg|_{\hat{x}_k} = \begin{bmatrix} \frac{-X}{\sqrt{X^2+Y^2+z^2}} & \frac{-Y}{\sqrt{X^2+Y^2+z^2}} & 0 \\ -\frac{zX}{\sqrt{X^2+Y^2}(X^2+Y^2+z^2)} & -\frac{zY}{\sqrt{X^2+Y^2}(X^2+Y^2+z^2)} & 0 \\ -\frac{Y}{X^2+Y^2} & \frac{X}{X^2+Y^2} & 0 \\ 0 & 0 & 1 \end{bmatrix}$$

$$R = \sqrt{(x_b - x)^2 + (y_b - y)^2 + z^2} \tag{17}$$

References

Manhães, Musa Morena Marcusso et al. (2016). "UUV Simulator: A Gazebo-based package for underwater intervention and multi-robot simulation". In: *OCEANS 2016 MTS/IEEE Monterey*, pp. 1–8. DOI: 10.1109/OCEANS.2016.7761080.